J Neuroimmune Pharmacol (2017) 12:544–554
DOI 10.1007/s11481-017-9744-7

ORIGINAL ARTICLE

Regulation of Cell Surface CB_2 Receptor during Human B Cell Activation and Differentiation

Julie T. Castaneda[1,2] · **Airi Harui**[1] · **Michael D. Roth**[1,2]

Received: 1 December 2016 / Accepted: 27 March 2017 / Published online: 31 March 2017

Abstract Cannabinoid receptor type 2 (CB_2) is the primary receptor pathway mediating the immunologic consequences of cannabinoids. We recently reported that human peripheral blood B cells express CB_2 on both the extracellular membrane and at intracellular sites, where-as monocytes and T cells only express intracellular CB_2. To better understand the pattern of CB_2 expression by human B cells, we examined $CD20^+$ B cells from three tissue sources. Both surface and intracellular expression were present and uniform in cord blood B cells, where all cells exhibited a naïve mature phenotype (IgD^+/$CD38^{Dim}$). While naïve mature and quiescent memory B cells (IgD^-/$CD38^-$) from tonsils and peripheral blood exhibited a similar pattern, tonsillar activated B cells (IgD^-/$CD38^+$) expressed little to no surface CB_2. We hypothesized that regulation of the surface CB_2 receptor may occur during B cell activation. Consistent with this, a B cell lymphoma cell line known to exhibit an activated phenotype (SUDHL-4) was found to lack cell surface CB_2 but express intracellular CB_2. Furthermore, in vitro activation of human cord blood resulted in a down-regulation of surface CB_2 on those B cells acquiring the activated phenotype but not on those retaining IgD expression. Using a CB_2 expressing cell line (293 T/CB_2-GFP), confocal microscopy confirmed the presence of both cell surface expression and multifocal intracellular expression, the latter of which co-localized with endoplasmic reticulum but not with mitochondria, lysosomes, or nucleus. Our findings suggest a dynamic multi-compartment expression pattern for CB_2 in B cells that is specifically modulated during the course of B cell activation.

Keywords Cannabinoids · Cannabinoid receptor CB2 · G protein-coupled receptors · Intracellular membrane receptors · B cells · B cell activation

Introduction

Cannabinoids, the primary bioactive constituents of marijuana, activate cannabinoid receptor type 1 (CB_1) and type 2 (CB_2) and signal through an endogenous human cannabinoid system to produce their biologic effects (Aizpurua-Olaizola et al. 2016; Cabral et al. 2015; Maccarrone et al. 2015; Pacher et al. 2006). Expression of CB_2 predominates in cells from the immune system (Castaneda et al. 2013; Schmöle et al. 2015), and cannabinoids have been described to exert potent immunosuppressive effects on antigen presenting cells (Klein and Cabral 2006; Roth et al. 2015), B cells and antibody production (Agudelo et al. 2008; Carayon et al. 1998), T cell responsiveness and cytokine production (Eisenstein and Meissler 2015; Yuan et al. 2002), and monocyte/macrophage function (Hegde et al. 2010; Roth et al. 2004). However, the majority of these findings stem from studies employing agonists and antagonists with defined CB_2 binding specificities, and only limited insight has been available regarding the actual expression patterns and dynamic regulation of CB_2 protein. CB_2 has traditionally been described as a seven-transmembrane G protein-coupled receptor (GPCR) expressed on the cell surface and responsive to extracellular ligand binding. Ligand binding has been shown to initiate both receptor internalization (Atwood et al. 2012) and a

✉ Michael D. Roth
mroth@mednet.ucla.edu

[1] Division of Pulmonary and Critical Care Medicine, Department of Medicine, CHS 37-131, David Geffen School of Medicine at UCLA, Los Angeles, CA 90095-1690, USA

[2] Inter-Departmental Program in Molecular Toxicology, University of California, Los Angeles, Los Angeles, CA 90095, USA

diverse number of intracellular signaling cascades, including adenylyl cyclase, cAMP, mitogen-activated protein (MAP) kinase, and intracellular calcium (Howlett 2005; Jean-Alphonse and Hanyaloglu 2011; Maccarrone et al. 2015). However, after using a highly sensitive and specific monoclonal anti-CB_2 antibody and fluorescent imaging, we were surprised to find that CB_2 was expressed exclusively in the intracellular compartment of human monocytes, dendritic cells, and T cells without detectable cell surface staining (Castaneda et al. 2013; Roth et al. 2015). Only human B cells expressed CB_2 on the cell surface, which internalized in response to ligand exposure, as well as within the intracellular compartment (Castaneda et al. 2013). These findings challenge our understanding of the CB_2 receptor and identify the need for additional insight.

It is not yet clear whether cannabinoids routinely bind and activate intracellular CB_2, but there is at least one report providing direct experimental evidence for this (Brailoiu et al. 2014). It is also not clear why B cells exhibit a receptor expression pattern that is distinct from other leukocytes or whether this is a unique feature in cells obtained from peripheral blood or related to the specific stage of cell activation or differentiation. B cell activation has been suggested to play a role in the pattern of CB_2 expression in a prior report (Carayon et al. 1998). In order to better understand CB_2 expression patterns exhibited by human B cells, this report examines cells obtained from three different tissue sources (adult peripheral blood, cord blood, and tonsils), evaluates the relationship between defined B cell subsets and CB_2 expression patterns, and uses an in vitro model for activating B cells in order to examine changes in CB_2 expression as they correlate to the life cycle of functional B cell responses.

Methods

Primary Cells and Cell Lines Following informed consent, peripheral blood leukocytes (PBL) were isolated by Ficoll-gradient centrifugation (GE HealthCare, Chicago, IL) from the blood of healthy human donors. Human umbilical vein cord blood leukocytes were obtained from anonymous donors through the UCLA Virology Core and isolated in the same manner. Fresh human tonsillar tissue was also obtained in an anonymous manner through the UCLA Translational Pathology Core from patients undergoing routine elective tonsillectomies. Tonsillar tissue was handled in a sterile manner, minced, and then extruded through a sterile 100 μm filter to produce single cells. Filtered cells were then rinsed with PBS (Cellgro, Manassas, VA) and processed in the same manner as PBL. Cell subsets were identified by flow cytometry using fluorescent-labeled monoclonal antibodies (mAb) directed against T cells (anti-CD3, Invitrogen, Camarillo, CA), B cells (anti-CD20, BD Biosciences, San Jose, CA), and B cell subsets (anti-IgD and anti-IgM, Biolegend, San Diego, CA and anti-CD27 and anti-CD38, BD Biosciences).

The human B cell non-Hodgkin's lymphoma cell line, SUDHL-4 (gifted by Dr. John Timmerman, UCLA) was cryopreserved, and when needed, it was cultivated in suspension in complete medium composed of RPMI-1640 (Cellgro) supplemented with 10% fetal bovine serum (Omega Scientific, Tarzana, CA), 50 μM 2-mercaptoethanol (MP Biomedicals, Santa Ana, CA), and 1% antibiotic-antimycotic solution (Cellgro).

Detection of CB_2 Receptor by Flow Cytometry CB_2 on the extracellular membrane was detected as previously described (Castaneda et al. 2013). In summary, cells were pre-treated with human AB Serum (Omega Scientific) followed by a 30 min incubation with unlabeled primary mouse IgG_2 mAb directed against either human CB_2 (clone #352114, 0.5 μg/tube, R&D Systems, Minneapolis, MN) or with an isotype-matched mAb against an irrelevant antigen, mouse NK1.1 (clone #PK136, 0.5 μg/tube, BD Biosciences), to assess non-specific background staining. After washing, cells that had been stained in this manner were incubated with an APC-labeled goat anti-mouse F(ab')2 mAb (APC-labeled GAM, 0.5 μg/tube, Invitrogen) for 30 min. To identify different leukocyte subsets, cells were incubated with lineage-specific fluorescent-labeled mAb for 20 min and washed. All cells were then fixed with 1% paraformaldehyde (Sigma-Aldrich, St. Louis, MO) and washed. Samples were protected from light and stored at 4 °C until analyzed.

In order to detect total cellular CB_2 expression (intracellular plus cell membrane), cell suspensions were fixed (1% paraformaldehyde), permeabilized (Permeabilizing Solution 2, BD Biosciences), and blocked with human AB serum. Staining with primary unlabeled mAb (against CB_2 or NK1.1) and secondary APC-labeled GAM were carried out as already detailed except for the use of a 60 min incubation time and the presence of permeabilizing solution. After washing, leukocytes were further stained with fluorescent-labeled antibodies as indicated for individual experiments, fixed, and stored for analysis.

In order to identify total cellular CB_2 expression in specific B cells subsets, cells were pre-stained with B cell subset markers (IgD, IgM, CD27, and CD38) prior to fixation, permeabilization, and staining for CB_2. This step prevented the labeling of intracellular subset markers which can otherwise result in misclassification. Cells were then fixed with 1% paraformaldehyde, washed, and cryopreserved in PBS with 2% human AB serum and 10% dimethyl sulfoxide (Sigma-Aldrich). On the day of CB_2 analysis, cells were rapidly thawed at 37 °C, treated with permeabilizing solution and stained for 30 min with either a directly-conjugated anti-CB_2 mAb (Alexa Fluor® 647-labeled mouse anti-human CB_2; clone #352114, 2 μg/tube, Novus Biologicals,

Littleton, CO) or with the corresponding isotype-matched and directly-conjugated anti-NK1.1 mAb (Alexa Fluor® 647-labeled anti-mouse NK1.1; clone #PK136, 2 μg/tube, Biolegend) to assess non-specific background staining. All cells were stained with fluorescent-labeled antibodies directed against CD20 and CD3 to promote gating and fixed once again with 1% paraformaldehyde prior to storage and analysis.

In Vitro Activation and Differentiation of Naïve Mature B Cells B cells obtained from umbilical vein cord blood were cultured for 5 days at 1×10^6 cells/mL in RPMI-1640 supplemented with 10% human AB serum and 1% antibiotic-antimycotic solution in combination with 5 μg/mL anti-IgM (Jackson ImmunoResearch, West Grove, PA), 100–250 ng/mL mega-CD40L (Enzo Life Sciences, Farmingdale, NY), 100 ng/mL IL-21 (Peprotech, Rocky Hill, NJ), and 100 ng/mL IL-4 (R&D Systems). Live leukocytes were gated based on their FSC vs SSC profile and phenotyped at day 0 (before culture) and day 2 to identify B cell subsets and to determine CB_2 expression as already described.

Multiparameter Flow Cytometry Multiparameter flow cytometry was carried out using a FACScan II-plus cytometer and SORP BD HTLSRII (BD Biosciences) with the acquisition of 5000–40,000 events depending upon the assay conditions. Analysis utilized FCS Express V3 or V5 software with gating on $CD20^+/CD3^-$ events followed by subset analyses (De Novo Software, Ontario, Canada). Flow cytometry results are presented as two-parameter dot plots with reported values representing the mean linear fluorescence intensity of the gated population.

Confocal Microscopy Pre-cleaned coverslips were coated overnight with 0.1 mg/mL poly-l-lysine hydrobromide (Sigma-Aldrich), washed with sterile culture water (Cellgro), and plated in 12 well plates with 1.5×10^5 293 T or 293 T/CB_2-GFP cells/mL for 48 h at 37 °C in complete medium composed of DMEM (Cellgro), 10% fetal bovine serum, and 1% antibiotic-antimycotic solution. For mitochondrial or lysosomal staining, cells were then washed with PBS and incubated with 150 nM MitoTracker® Orange CMTMRos (Molecular Probes, Eugene, OR) in serum free media or 100 nM LysoTracker® Red DND-99 (Molecular Probes) in complete medium for 2 h at 37 °C. Cells were then washed with pre-warmed DMEM or complete medium. MitoTracker-stained cells were fixed and incubated with 1% paraformaldehyde for 20 min at 4 °C before mounting. LysoTracker-stained cells were mounted and imaged immediately without fixation. For endoplasmic reticulum (ER)-staining, cells were fixed and incubated with 1% paraformaldehyde and treated with permeabilizing solution. Cells were incubated with 200 μg/mL Concanavalin A, Alexa Fluor® 594 (Molecular Probes) for 60 min in the dark at 4 °C. Cells were then washed with PBS with 2% human AB serum. ER-stained cells were mounted and imaged immediately without fixation. Coverslips were mounted onto slides with one drop of SlowFade® Diamond Antifade Mountant with DAPI (Molecular Probes). For co-localization studies, organelle-specific stained cells were fixed and incubated with 1% paraformaldehyde and treated with permeabilizing solution. Cells were washed and followed by a 30 min incubation with an Alexa Fluor® 647-labeled mAbs (against CB_2 or NK1.1). After washing, cells were fixed with 1% paraformaldehyde and mounted for image analysis. Slides were imaged on SP2 1P–FCS or SP5 Blue confocal microscopes in 10–20 sections.

Statistics A minimum of three replicate experiments were carried out for each assay. Flow cytometry dot-plots display results from a single representative tube of a single experiment. Values are expressed as mean fluorescent intensities (MFI) for each representative experiment. All other data are presented as means of replicate experiments as detailed. The difference between means was determined using a Wilcoxon Signed-Rank Test with $p < 0.05$ accepted as statistically significant.

Results

Heterogeneity of B Cell Populations and CB_2 Expression in Leukocytes Obtained from Cord Blood, Adult Peripheral Blood, and Tonsils In order to determine if surface expression of CB_2 is a uniform feature of all B cell populations or whether it varies with the local environment or state of differentiation, flow cytometry was used to examine the $CD20^+/CD3^-$ population recovered from three different sources, including umbilical vein cord blood, adult peripheral blood, and tonsils. IgD vs CD38 and IgD vs IgM profiles were assessed for all 3 sources of B cells. $CD20^+$ B cells recovered from cord blood exhibited a homogeneous phenotype consistent with naïve mature B cells ($IgD^+/CD38^{Dim}$), while cells recovered from peripheral blood exhibited markers suggestive of both naïve mature and quiescent memory ($IgD^-/CD38^-$) subsets. Cells recovered from tonsils demonstrated features of all three subsets: naïve mature, activated ($IgD^-/CD38^+$), and quiescent memory B cells (Fig. 1a). Similarly, staining with unconjugated anti-CB_2 mAb followed by secondary detection with APC-labeled GAM ranged from homogeneous and clearly positive on cord blood and peripheral blood B cells to heterogeneous, with cells that appeared positive and others that appeared negative, on tonsillar B cells. Cells that had been stained under the same conditions with mAb directed against an irrelevant antigen, mouse NK1.1, followed by APC-labeled GAM were used to measure non-specific background staining and to set the threshold for distinguishing between

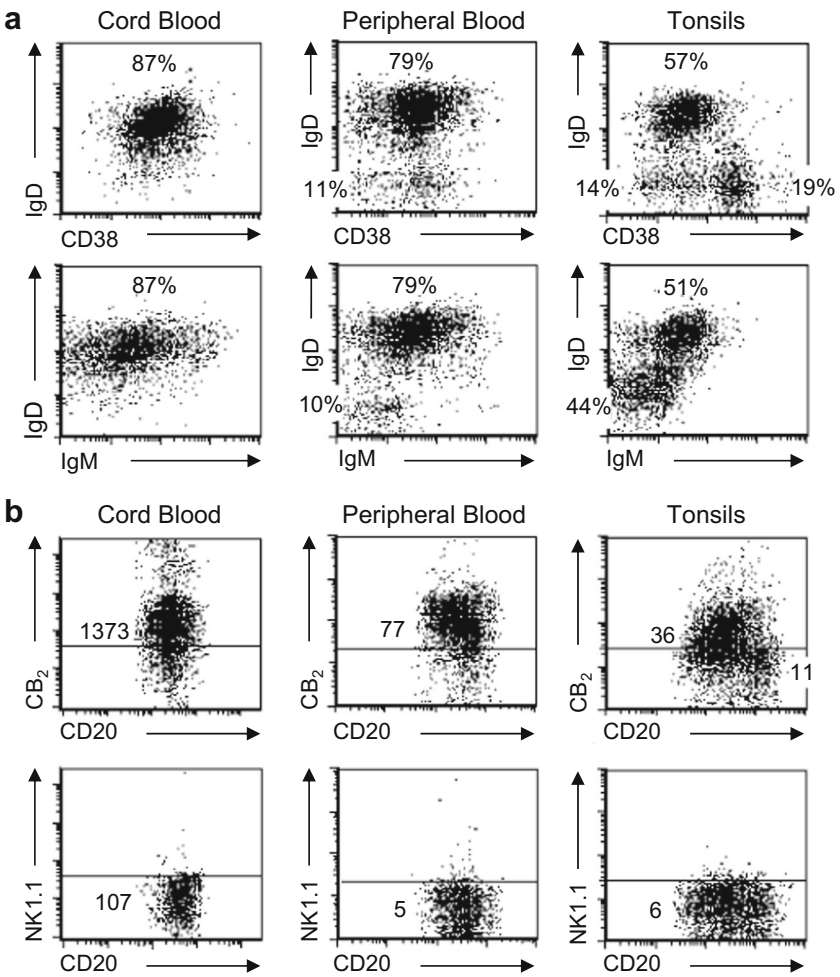

Fig. 1 Heterogeneity of B cell populations and CB_2 expression in leukocytes obtained from cord blood, adult peripheral blood, and tonsils (**a**) Leukocytes from umbilical vein cord blood, peripheral blood, and tonsils were stained with fluorescent mAb and gated to express only viable events within the $CD20^+/CD3^-$ B cell region. 5-color staining was used to identify the distribution of cells exhibiting IgD and IgM, expressed only on naïve mature B cells, and CD38, which is dim on naïve mature B cells, positive on activated B cells, and dim/negative on quiescent memory B cells. Percentages for each population are listed. **b** Cells within the $CD20^+/CD3^-$ gate were also evaluated for expression of extracellular CB_2 using a primary unlabeled mAb against CB_2 protein followed by secondary staining with APC-labeled GAM. Background staining (horizontal line) was set by staining cells with an unlabeled isotype-matched irrelevant target (anti-mouse NK1.1) followed by secondary staining with APC-labeled GAM. Numbers represent relative MFI for staining on the Y axis. Representative experiment shown, $n = 6$

positive and negative CB_2 expression (Fig. 1b). Consistent with our prior findings with peripheral blood, no surface CB_2 staining was observed on $CD3^+$ T cells regardless of the source of cells (data not shown).

Surface Expression of CB_2, but Not Total Cellular CB_2, is Limited in Activated B Cells Recovered from Tonsils In order to directly examine the relationship between B cell subsets and CB_2 expression, gated $CD20^+/CD3^-$ B cells from human tonsils were classified into three defined subsets (naïve mature, activated, and quiescent memory; Fig. 2a) and evaluated for both surface expression and total cellular CB_2 expression by flow cytometry (Fig. 2b). In these experiments, both the anti-CB_2 mAb and the anti-NK1.1 mAb, to detect non-specific background staining, were directly conjugated with Alexa Fluor® 647. This detailed subset analysis clarified that the expression of CB_2 that occured on the surface of both naïve mature ($IgD^+/CD38^{Dim}$) and quiescent memory ($IgD^-/CD38^-$) subsets was relatively homogeneous and strongly-positive, while surface CB_2 expression on the surface of the activated subset ($IgD^-/CD38^+$) ranged from negative to dim-positive. Compared to the MFI for CB_2 expression by the naïve mature B cell subset, average MFI expression by the activated B cell subset was reduced to only 32 ± 10% ($p < 0.05$), while MFI expression by the quiescent memory B cell subset averaged 149 ± 73% ($p > 0.05$; mean ± SD, $n = 6$ experiments). When cells were permeabilized to detect total cellular expression of CB_2 (intracellular plus cell membrane), all three B cell subsets exhibited high expression of CB_2 with the highest expression by the activated subset. When compared to the MFI for intracellular CB_2 expression by naïve mature B cells, expression by activated B cells represented 205 ± 69% of this population, while expression by quiescent memory B cells represented 107 ± 5% (mean ± SD, $n = 3$ experiments).

Malignant B Cell Lines Expressing an Activated Phenotype Exhibit the Same Pattern of CB_2 Expression as that Observed with Primary Activated B Cells from Tonsils CB_2 has been described as an oncogene with enhanced expression of CB_2 by leukemia and lymphoma cell lines (Jorda et al. 2003; Pérez-Gómez et al. 2015). Given the expression pattern observed with tonsillar B cells, we hypothesized that altered CB_2 expression might be associated with an activated phenotype and that expression by these cells might

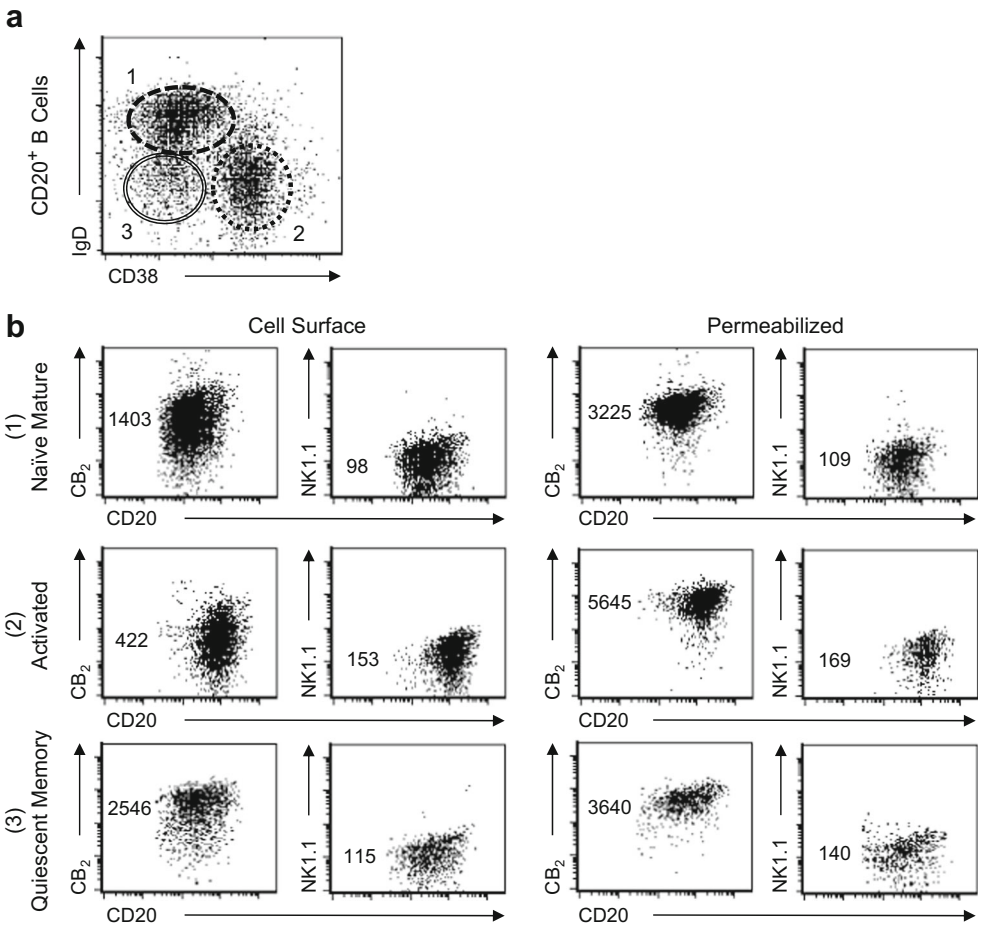

Fig. 2 Surface expression of CB_2, but not total cellular CB_2, is limited in activated B cells recovered from tonsils (**a**) B cells within the gate for viable $CD20^+/CD3^-$ events obtained from mechanically-digested human tonsils were classified into three subsets based on IgD and CD38 expression patterns: (#1) naïve mature, (#2) activated, and (#3) quiescent memory. **b** B cells within each of these three subset classifications (#1 - #3, correspondingly) were then stained with either Alexa Fluor® 647-labeled mouse IgG2a mAb directed against either human CB_2 or mouse NK1.1 (isotype control) while still viable, facilitating detection of cell surface expression (left panel, $n = 6$), or after being fixed and permeabilized for the detection of total cellular expression (right panel, $n = 3$). Numbers represent relative MFI for staining on the Y axis. Representative experiment shown

reside primarily at an intracellular location. A B cell lymphoma cell line described as exhibiting the characteristics of activated B cells, SUDHL-4, was therefore assessed for both B cell subset markers, IgD, CD38, and CD27 (Fig. 3a), and for cell surface (Fig. 3b) and total CB_2 expression (Fig. 3c) using unconjugated anti-CB_2 or anti-NK1.1 mAb followed by APC-labeled GAM. As expected for the activated phenotype, these cells were $IgD^-/CD38^+/CD27^+$ (tonsillar activated B cells were also $CD27^+$, data not shown). Following the same pattern as activated B cells from tonsils, SUDHL-4 cells did not express cell surface CB_2, but exhibited high total cellular CB_2 after being fixed, permeabilized, and stained with anti-CB_2 mAb. Similar findings were observed with two other human malignant B cell lymphomas tested (Ramos and Granta-519 cells, data not shown).

Changes in CB_2 Expression when Human Naïve B Cells are Activated in Vitro and Acquire the Phenotype of Activated B Cells The difference in CB_2 expression between activated B cells and other subsets lead us to hypothesize that CB_2 expression is modulated as part of the activation process. In order to directly test this hypothesis, cord blood B cells were activated by cross-linking the B cell receptor in combination with mega-CD40L, anti-IgM, IL-21, and IL-4 as physiologic costimulatory signals. Activation was assessed by changes in expression of cell surface IgD, CD27, and CD38. At day 0, B cells start out in a naïve mature state ($IgD^+/CD38^{Dim}$). At day 2, two distinct sub-populations emerge, one still phenotypically naïve (IgD^+) and the other with an activated phenotype (IgD^-). At day 2, both populations express the CD27 B cell activation marker consistent with their exposure to cytokines and receptor targeted antibodies (Fig. 4a). Each population was then examined for the expression of both cell surface CB_2 and total cellular CB_2 using Alexa Fluor® 647-conjugated anti-CB_2 or anti-NK1.1 mAbs. On day 0, cell surface CB_2 expression was obviously positive as was intracellular expression. Similarly, the B cells that remained phenotypically naïve on day 2 (retention of IgD expression) exhibited both cell surface and intracellular CB_2. However, surface expression of CB_2 decreased on those day 2 cells that simultaneously lost IgD expression and gained expression of CD27, consistent with having acquired a fully-activated phenotype. As was the case with activated B cells recovered from tonsils, the activated cells generated in vitro still exhibited intracellular CB_2 even though surface expression had been lost (Fig. 4b).

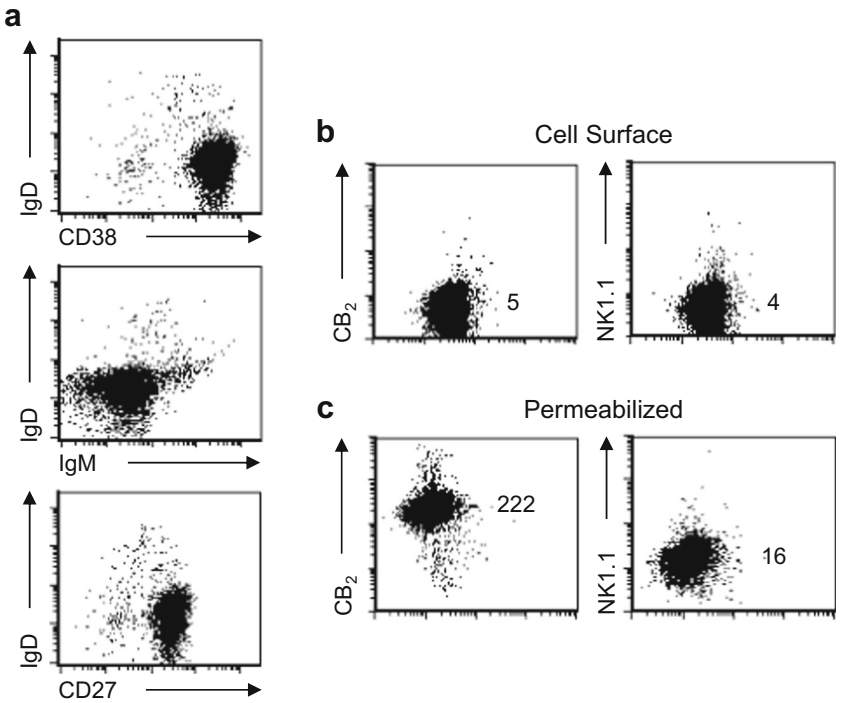

Fig. 3 A malignant B cell line expressing an activated phenotype exhibits the same pattern of CB_2 expression as that observed with primary activated B cells from tonsils (**a**) Cells from the malignant B cell lymphoma cell line, SUDHL-4, exhibited cell surface markers consistent with an activated B cell subset based on the expression pattern for IgD (negative), CD38 (positive), and CD27 (positive). **b** Cells were stained while still viable for detection of cell surface CB_2 with a primary unlabeled mAb against CB_2 protein or isotype control, NK1.1, and then stained with APC-labeled GAM. **c** For total cell expression of CB_2, cells were fixed and permeabilized prior to specific staining. Numbers represent relative MFI for staining on the Y axis. Representative experiment shown, $n = 3$

Intracellular CB_2 is Expressed in a Diffuse but Punctate Pattern and Demonstrates Co-Localization with Endoplasmic Reticulum Compartments As an integral transmembrane GPCR, CB_2 has classically been viewed as a cell surface receptor. However, the current findings suggest that it is the intracellular form of CB_2 that represents the most consistent and predominant form. Confocal microscopy was therefore employed to investigate the distribution and location of intracellular CB_2 in peripheral blood B cells, the activated B cell lymphoma cell line, SUDHL-4, and in a 293 T cell line transduced to stably express CB_2 (293 T/CB_2-GFP). Detection employed the Alexa Fluor® 647-conjugated anti-CB_2 mAb. An identical appearing diffuse, but punctate, cytoplasmic distribution of CB_2 was observed in all three cases (Fig. 5a). Cells stained in an identical manner using the Alexa Fluor® 647-conjugated isotype control NK1.1 mAb exhibited no detectible fluorescence (data not shown). In order to compare expression patterns to other organelle markers, cells from the 293 T/CB_2-GFP line were also stained with Concanavalin A-Alexa Fluor® 594, MitoTracker® Orange CMTMRos, and LysoTracker® Red DND-99 reagents to determine ER, mitochondrial, and lysosomal staining patterns, respectively (Fig. 5b). Lysosomal staining shared no obvious features with the staining pattern for CB_2, but the ER and mitochondrial staining also exhibited a diffuse but punctate pattern. Given prior evidence that Δ-9-tetrahydrocanabinol (THC), a prototypic cannabinoid that binds to the CB_2 receptor, has potent effects on cell energetics and mitochondrial membrane potential (Sarafian et al. 2003) and that activation of CB_2 promotes endoplasmic reticulum stress (Salazar et al. 2009), co-localization studies were carried out to assess whether CB_2 is expressed in mitochondrial and/or ER membranes (Fig. 5c). Despite some similarity in staining pattern, no fluorescent co-localization was observed when mitochondrial and CB_2 staining were imaged together in the 293 T/CB_2-GFP cell line. However, extensive co-localization of fluorescent images was observed when dual staining for ER and CB_2 was carried out in cells from the 293 T/CB_2-GFP line and imaged by confocal microscopy. An identical pattern of co-localization was also observed between the CB_2 receptor and ER staining, but not CB2 and mitochondrial staining, in the SUDHL-4 cell line (data not shown). Cell surface CB_2 also co-localized with cell membrane markers when assessed in the 293 T/CB_2-GFP line (data not shown).

Discussion

The concept of CB_2 as a simple GPCR expressed on the surface of human leukocytes (Graham et al. 2010; Klein et al. 2003) is being challenged by a number of recent findings, including our

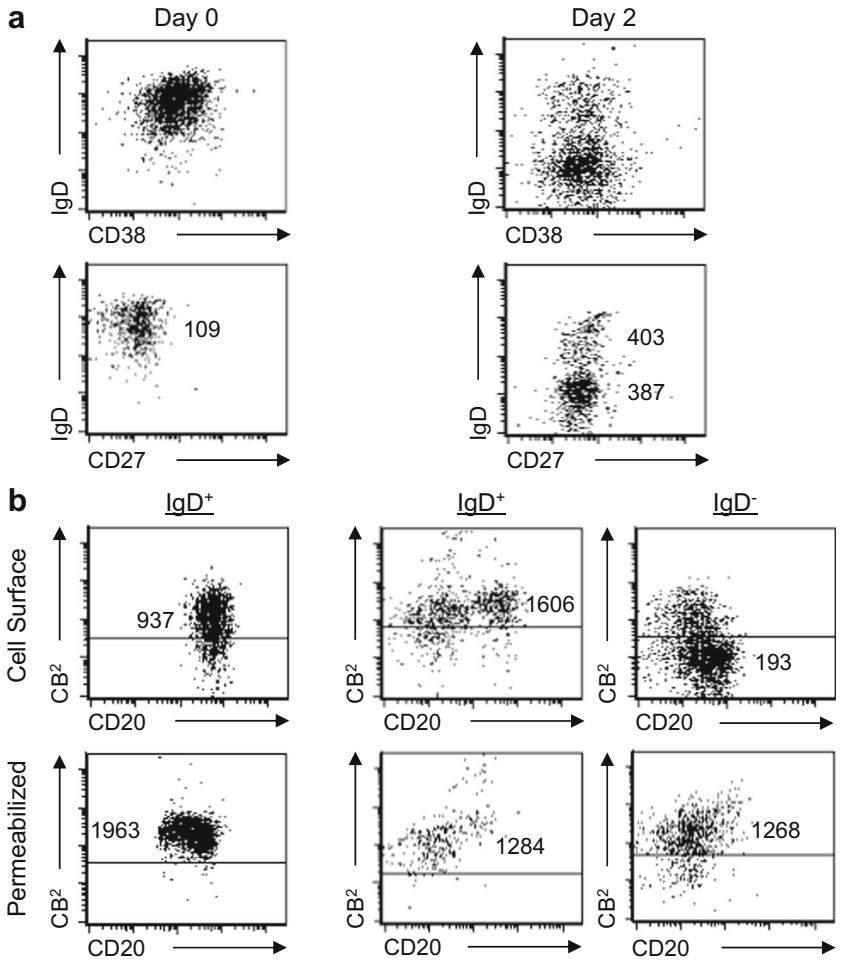

Fig. 4 Changes in CB_2 expression when human naïve B cells are activated in vitro and acquire the phenotype of activated B cells (**a**) 1×10^6 umbilical vein cord blood B cells/mL were cultured for 2 days at 37 °C and activated in vitro by addition of 100 ng/mL IL-21, 100–250 ng/mL mega-CD40L, 5 μg/mL anti-IgM, and 100 ng/mL IL-4 in complete medium. Fresh resting cells (day 0) and activated cells (day 2) were gated on the viable $CD20^+/CD3^-$ population and analyzed by flow cytometry for the expression of subset markers to identify naïve mature B cells ($IgD^+/CD38^{Dim}$) and activated B cells ($IgD^-/CD38^+$). The IgD vs CD27 profile was also assessed. Numbers represent relative MFI for staining on the Y axis. **b** Gated cells exhibiting the phenotype of either naïve (IgD^+) or activated (IgD^-) B cells were then independently evaluated for fluorescence produced by an Alexa Fluor® 647-conjugated anti-CB_2 mAb. Live cells were gated based on FSC vs SSC profile and were stained to measure cell surface staining while total cell expression of CB_2 (intracellular plus cell membrane) was determined in cells that were fixed and permeabilized prior to CB_2 staining. Numbers represent relative MFI for staining on the Y axis. Representative experiment shown, $n = 6$

imaging studies that employ a mAb against the N-terminal domain of CB_2 to detect protein expression (Castaneda et al. 2013; Roth et al. 2015). Using a combination of multi-parameter flow cytometry and flow-based imaging, we observed that CB_2 can be expressed on the cell surface, as expected, but is also present within the cytoplasm. Furthermore, the expression pattern for CB_2 was not uniform across cell types. The intracellular expression, rather than the extracellular expression, was the predominant form (Castaneda et al. 2013). While peripheral blood B cells expressed both cell surface and intracellular CB_2, T cells, monocytes, and dendritic cells exhibited only the intracellular form of CB_2. Even though cell surface CB_2 can rapidly internalize when exposed to a ligand, the distribution of this internalized CB_2 did not appear to account for the pre-existing distribution of intracellular CB_2. The biologic basis underlying these different CB_2 expression patterns has not yet been fully delineated, but there is growing evidence that the presence of GPCRs at different cellular locations is an important feature of these receptors that promotes functional heterogeneity with respect to downstream signaling and biologic responses (Flordellis 2012; Gaudet et al. 2015). Along these lines, there is growing evidence that intracellular forms for both CB_1 and CB_2 are common and exert distinct biologic effects (Brailoiu et al. 2011, 2014; Bernard et al. 2012). In this setting, understanding the distribution, regulation, and dynamic balance between cell surface and intracellular CB_2 receptors is likely to provide important insight regarding cannabinoid receptor biology.

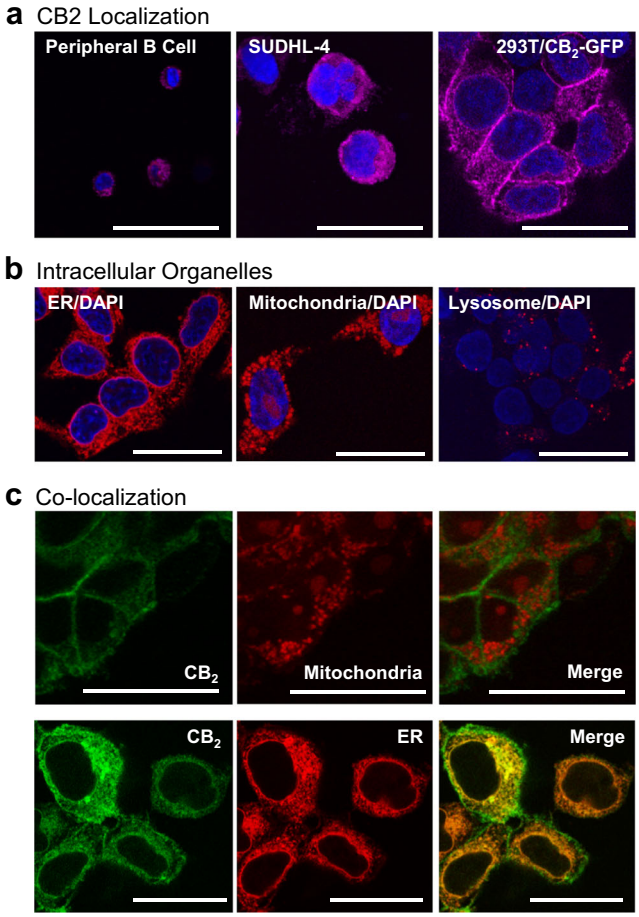

Fig 5 Intracellular CB_2 is expressed in a diffuse but punctate pattern and demonstrates co-localization with endoplasmic reticulum compartments (**a**) $CD20^+/CD3^-$ B cells purified from peripheral blood, cells prepared from the SUDHL-4 lymphoma cell line, and 293 T/CB_2-GFP cells were fixed, permeabilized, and stained with an Alexa Fluor® 647-conjugated mAb against CB_2 protein (displayed as magenta) and mounted with SlowFade® Diamond Antifade Mountant with DAPI (blue) prior to examination by confocal fluorescence microscopy. Magnification 63X; Scale Bar 25 μm;10–20 sections/cell with an SP5 blue confocal microscope. **b** 293 T/CB_2-GFP cells were grown on poly-l-lysine coated coverslips, fixed, permeabilized and stained with either Concanavalin A (ER, red), MitoTracker (mitochondria, red), or LysoTracker (lysosome, red) prior to mounting with SlowFade® Diamond Antifade Mountant with DAPI (blue). CB_2 and mitochondrial stained cells were fixed with 1% paraformaldehyde for 20 min at 4 °C and later imaged. ER and lysosomal stained cells were imaged immediately without fixation. Cells were imaged in 10–20 sections with an SP5 blue confocal microscope. Magnification 63X; Scale Bar 25 μm. **c** For co-localization imaging with mitochondrial markers, 293 T-CB_2-GFP cells grown on poly-l-lysine coated coverslips were first stained with MitoTracker (red) for 2 h at 37 °C, then fixed, permeabilized, and stained with anti-CB_2 mAb (green) for 30 min at 4 °C. Cells were fixed, mounted and imaged in 10–20 sections with an SP5 blue confocal microscope (top). For co-localization with ER markers, 293 T-CB_2-GFP cells grown on poly-l-lysine coated coverslips were fixed, permeabilized, and stained with anti-CB_2 mAb (green) and Concanavalin A (red) for 60 min at 4 °C. Cells were immediately mounted without fixation and imaged in 10–20 sections with an SP5 blue confocal microscope (bottom). Magnification 63X; Scale bar 25 μm

The unique expression of CB_2 on the surface of peripheral blood B cells led us to question whether this represented an intrinsic and stable feature of B cells in general or was more characteristic of those in peripheral blood. B cells were therefore obtained from three sources for comparison including umbilical vein cord blood, adult peripheral blood, and tonsils. B cell subsets from these different sources were characterized as either naïve mature, activated, or quiescent memory B cells based on their expression of IgD, IgM, CD27, and CD38 (Ettinger et al. 2005). When analyzed in this manner, it became clear that all naïve and quiescent memory B cells, regardless of source, expressed both cell surface and intracellular CB_2. On the other hand, B cells with an activated phenotype ($IgD^-/IgM^-/CD38^+/CD27^+$) expressed primarily the intracellular form of CB_2 (with minimal to no surface staining), and in most cases the level of intracellular CB_2 was higher than that observed in naïve or memory B cells obtained from the same sample. Prior studies had noted that $IgD^-/CD38^+$ germinal center B cells, consistent with the activated tonsillar B cells studied here, express a different pattern of CB_2 protein staining than other B cells (Carayon et al. 1998; Rayman et al. 2004). However, that study used a polyclonal rabbit antibody that targeted a C-terminal CB_2 peptide sequence and concluded that their findings represented the transition of CB_2 from an inactive to an "activated/phosphorylated" state. It is plausible that their findings actually mirrored ours, but features related to differences in receptor localization were not appreciated due to differences in techniques.

Given the unique CB_2 signature of the activated B cell population, we entertained two possible hypotheses based on the existing literature. The simplest hypothesis being that B cell activation is associated with a down-regulation of the surface CB_2 receptor. Alternatively, it has been reported that CB_2 can form heterodimers with the CXCR4 chemokine receptor and has chemotactic properties that result in the selective homing of CB_2^+ and CB_2^- B cells to different regions of lymphoid follicles (Basu et al. 2013; Coke et al. 2016). We addressed the potential linkage between B cell activation and CB_2 expression using two different approaches. CB_2 is known to be expressed by B cell lymphomas and has been described as an oncogene (Jorda et al. 2003; Pérez-Gómez et al. 2015). We therefore examined a human B cell lymphoma cell line, SUDHL-4, that had been described to express an activated B cell phenotype. Consistent with a linkage between activation state and CB_2 expression pattern, this cell line and two other lymphoma lines that exhibited an "activated" phenotype were found to exhibit high intracellular CB_2 but no surface staining. In order to more directly test the linkage between B cell activation and CB_2 expression pattern, we employed an in vitro model in which naïve mature human B cells obtained from umbilical vein cord blood were activated with a combination of receptor signaling and supporting cytokines (Ettinger et al. 2005). After 5 days in culture, the initial homogeneous population of naïve B cells had evolved into two obvious subsets:

one that retained the naïve B cell phenotype (IgD^+) and the other that exhibited an activated B cell phenotype (IgD^-). When examined for the expression of CB_2, there was a clear distinction between these two subsets with a loss of extracellular CB_2 only on the activated subset. Collectively, the evidence presented in this report points to a clear linkage between the acquisition of an "activated" B cell phenotype and specific regulation of CB_2 protein expression.

With limited information regarding the nature of intracellular CB_2, we employed a combination of confocal microscopy and marker co-localization studies to evaluate the distribution and location of intracellular CB_2. It exhibited a diffuse but punctate pattern within the cytoplasm. This appearance was the same regardless of the type of cells studied – primary peripheral blood B cells, the SUDHL-4 cell line, or the 293 T/CB_2-GFP cell line that we had previously described (Castaneda et al. 2013). Using the 293 T/CB_2-GFP cell line, we compared the distribution of CB_2 staining to the staining of ER, mitochondrial, and lysosomal markers. The sparse and well defined features of lysosomal staining did not match and were not pursued further. On the other hand, the punctate but diffuse pattern of ER and mitochondrial staining shared some similarities to the pattern observed with CB_2. These represented interesting observations given our prior findings that THC can disrupt cell energetics and mitochondrial transmembrane potential in airway epithelial cells in a CB_2-dependent manner (Sarafian et al. 2003, 2008) and evidence that intracellular CB_1 receptors might be expressed on subset of mitochondria in hippocampal neurons (Bernard et al. 2012). However, we noted no obvious co-localization between the CB_2 receptor and mitochondrial markers when directly examined by dual staining and confocal microscopy. There has also been considerable interest in the effects of cannabinoids and CB_2 activation on endoplasmic reticulum stress-related targets that mediate autophagy, apoptosis, and cell death in CB_2-expressing cancer cells (Salazar et al. 2009; Hernández-Tiedra et al. 2016). Interestingly, our studies do identify extensive co-localization between the CB_2 receptor and an ER marker in both 293 T/CB_2-GFP and SUDHL-4 cells when directly examined by dual staining and confocal microscopy. The presence of CB_2 receptors in ER compartments may suggest alternative splice forms that do not traffic to the cell membrane yet contribute to the diversity of receptor signaling and ligand responses that are observed with cannabinoids. The recent studies by Brailoiu et al. (2014) provide striking evidence that cannabinoids can induce both calcium influx through the cell membrane and the release of calcium from intracellular stores and that these responses result from CB_2 receptor activation at different cellular locations. In that work, which employed the malignant U2OS human osteosarcoma cell line expressing a CB_2-β-arrestin2-GFP gene construct, CB_2 protein and calcium release were localized to endolysosomes utilizing a combination of functional and imaging studies. Our studies have not yet addressed the presence of signaling or the functional role of the extensive CB_2 receptor expression observed in the ER compartment.

In summary, we can conclude that the expression of CB_2 in human leukocytes appears to be specifically regulated with respect to the cellular location (cell membrane versus intracellular distribution), the cell lineage being studied (B cells as compared to T cells, monocytes, and dendritic cells), and the state of B cell activation and differentiation (activated versus the naïve and memory subsets). The presence of an activated phenotype on B cells is specifically associated with down-regulation of the surface CB_2 receptor, a feature identified in B cells recovered from human tonsils and also observed in vitro when naïve B cells were stimulated to acquire an activated phenotype. Given the capacity for cell surface CB_2 to form heterodimers with chemokine receptors and promote migration and homing and given the location of CB_2^+ and CB_2^- B cells in different compartments within lymphoid follicles (Basu et al. 2013; Coke et al. 2016), it is possible that modulating surface CB_2 during B cell activation plays an important role in trafficking. The capacity for T cells, dendritic cells, and malignant B cells to respond to cannabinoids in a CB_2-dependent manner has been well characterized (McKallip et al. 2002; Roth et al. 2015; Yuan et al. 2002), yet these cells do not express CB_2 on the cell surface. The logical conclusion is that intracellular CB_2 must also be capable of mediating ligand-induced signaling and biological consequences. With the recent report by Brailoiu et al. (2014), there is now direct evidence for this. Given the high membrane solubility of cannabinoids, we hypothesize that the presence of CB_2 at different locations within a cell provides a mechanism for cells to link receptor activation to different signaling and biologic consequences, resulting in an expanded functional heterogeneity of cannabinoids. The specific role of different receptors on biologic function remains to be determined but will likely be very informative in understanding cannabinoid biology.

Acknowledgements Research reported in this publication was supported by the National Institute on Drug Abuse, National Institutes of Health, under award numbers 5-R01-DA037102. JT Castaneda was supported by a Ruth L. Kirschstein National Research Service Award (NRSA) Individual Predoctoral Fellowship to Promote Diversity in Health-Related Research from the National Institute on Drug Abuse, National Institutes of Health, under award numbers 1 F31 DA036293 and by a North American Graduate Fellowship Award from the American College of Toxicology. Flow cytometry was performed in the UCLA Jonsson Comprehensive Cancer Center (JCCC) and Center for AIDS Research (CFAR) Flow Cytometry Core Facility that is supported by National Institutes of Health awards CA-16042 and AI-28697, and by the JCCC, the UCLA AIDS Institute, and the David Geffen School of Medicine at UCLA. Confocal laser scanning microscopy was performed at the CNSI Advanced Light Microscopy/Spectroscopy Shared Resource Facility at UCLA, supported with funding from NIH-NCRR shared resources grant (CJX1-443835-WS-29646) and NSF Major Research Instrumentation grant (CHE-0722519). Cord blood mononuclear cells derived from anonymized donors were obtained from the CFAR Virology Core Lab that is supported by the National Institutes of Health Award AI-28697 and by the UCLA AIDS Institute and the UCLA Council of Bioscience Resources.

Compliance with Ethical Standards

Conflict of Interest The authors declare that they have no conflict of interest.

Ethical Approval All procedures performed in studies involving human participants were in accordance with the ethical standards of the institutional and/or national research committee and with the 1964 Helsinki declaration and its later amendments or comparable ethical standards.

References

Agudelo M, Newton C, Widen R, Sherwood T, Nong L, Friedman H, Klein TW (2008) Cannabinoid receptor 2 (CB2) mediates immunoglobulin class switching from IgM to IgE in cultures of murine-purified B lymphocytes. J NeuroImmune Pharmacol 3(1):35–42. doi:10.1007/s11481-007-9088-9

Aizpurua-Olaizola O, Elezgarai I, Rico-Barrio I, Zarandona I, Etxebarria N, Usobiaga A (2016) Targeting the endocannabinoid system: future therapeutic strategies. Drug Discov Today. doi:10.1016/j.drudis.2016.08.005

Atwood B, Wager-Miller J, Haskins C, Straiker A, Mackie K (2012) Functional selectivity in CB2 receptor signaling and regulation: implications for the therapeutic potential of CB2 ligands. Mol Pharmacol 81(2):250–263. doi:10.1124/mol.111.074013

Basu S, Ray A, Dittel BN (2013) Cannabinoid receptor 2 (CB2) plays a role in the generation of germinal center and memory B cells, but not in the production of antigen-specific IgG and IgM, in response to T-dependent antigens. PLoS One 8(6): e67587. doi:10.1371/journal.pone.0067587

Bernard G, Massa F, Puente N, Lourenco J, Bellocchio L, Soria-Gomez E, Matias I, Delamarre A, Metna-Laurent M, Cannich A, Hebert-Chatelain E, Mulle C, Ortega-Gutierrez S, Martin-Fontecha M, Klugmann M, Guggenhuber S, Lutz B, Gertsch J, Chaouloff F, Lopez-Rodriguez ML, Grandes P, Rossignol R, Marsicano G (2012) Mitochondrial CB1 receptors regulate neuronal energy metabolism. Nat Neurosci 15:558–564. doi:10.1038/nn.3053

Brailoiu GC, Deliu E, Marcu J, Hoffman NE, Console-Bram L, Zhao P, Madesh M, Abood ME, Brailoiu E (2014) Differential activation of intracellular versus plasmalemmal CB2 cannabinoid receptors. Biochemistry 53(30):4990–4999. doi:10.1021/bi500632a

Brailoiu GC, Oprea TI, Zhao P, Abood ME, Brailoiu E (2011) Intracellular cannabinoid type 1 (CB1) receptors are activated by anandamide. J Biol Chem 286:29166–29174. doi:10.1074/jbc.M110.217463

Cabral GA, Rogers TJ, Lichtman AH (2015) Turning over a new leaf: cannabinoid and endocannabinoid modulation of immune function. J NeuroImmune Pharmacol 10(2):193–203. doi:10.1007/s11481-015-9615-z

Carayon P, Marchand J, Dussossoy D, Derocq JM, Jbilo O, Bord A, Bouaboula M, Galiègue S, Mondière P, Pénarier G, Fur GL, Defrance T, Casellas P (1998) Modulation and functional involvement of CB2 peripheral cannabinoid receptors during B-cell differentiation. Blood 92(10):3605–3615

Castaneda JT, Harui A, Kiertscher SM, Roth JD, Roth MD (2013) Differential expression of intracellular and extracellular CB_2 cannabinoid receptor protein by human peripheral blood leukocytes. J NeuroImmune Pharmacol 8(1):323–332. doi:10.1007/s11481-012-9430-8

Coke CJ, Scarlett KA, Chetram MA, Jones KJ, Sandifer BJ, Davis AS, Marcus AI, Hinton CV (2016) Simultaneous activation of induced Heterodimerization between CXCR4 chemokine receptor and cannabinoid receptor 2 (CB2) reveals a mechanism for regulation of tumor progression. J Biol Chem 291(19):9991–10005. doi:10.1074/jbc.M115.712661

Eisenstein TK, Meissler JJ (2015) Effects of cannabinoids on T-cell function and resistance to infection. J NeuroImmune Pharmacol 10(2): 204–216. doi:10.1007/s11481-015-9603-3

Ettinger R, Sims GP, Fairhurst AM, Robbins R, da Silva YS, Spolski R, Leonard WJ, Lipsky PE (2005) IL-21 induces differentiation of human naïve and memory B cells into antibody-secreting plasma cells. J Immunol 175(12):7867–7879. doi:10.4049/jimmunol.175.12.7867

Flordellis CS (2012) The plasticity of the 7TMR signaling machinery and the search for pharmacological selectivity. Curr Pharm Des 18(2): 145–160. doi:10.2174/138161212799040556

Gaudet HM, Cheng SB, Christensen EM, Filardo EJ (2015) The G-protein coupled estrogen receptor, GPER: the inside and inside-out story. Mol Cell Endocrinol 418(Pt 3):207–219. doi:10.1016/j.mce.2015.07.016

Graham ES, Angel CE, Schwarcz LE, Dunbar PR, Glass M (2010) Detailed characterization of CB2 receptor protein expression in peripheral blood immune cells from healthy human volunteers using flow cytometry. Int J Immunopathol Pharmacol 23(1):25–34

Hegde VL, Nagarkatti M, Nagarkatti PS (2010) Cannabinoid receptor activation leads to massive mobilization of myeloid-derived suppressor cells with potent immunosuppressive properties. Eur J Immunol 40(12):3358–3371. doi:10.1002/eji.201040667

Hernández-Tiedra S, Fabriàs G, Dávila D, Salanueva ÍJ, Casas J, Montes LR, Antón Z, García-Taboada E, Salazar-Roa M, Lorente M, Nylandsted J, Armstrong J, López-Valero I, McKee CS, Serrano-Puebla A, García-López R, González-Martínez J, Abad JL, Hanada K, Boya P, Goñi F, Guzmán M, Lovat P, Jäättelä M, Alonso A, Velasco G (2016) Dihydroceramide accumulation mediates cytotoxic autophagy of cancer cells via autolysosome destabilization. Autophagy 12(11):2213–2229. doi:10.1080/15548627.2016.1213927

Howlett AC (2005) Cannabinoid receptor signaling. Handb Exp Pharmacol 168:53–79. doi:10.1007/3-540-26573-2_2

Jean-Alphonse F, Hanyaloglu AC (2011) Regulation of GPCR signal networks via membrane trafficking. Mol Cell Endocrinol 331(2): 205–214. doi:10.1016/j.mce.2010.07.010

Jorda MA, Rayman N, Valk P, De Wee E, Delwel R (2003) Identification, characterization, and function of a novel oncogene: the peripheral cannabinoid receptor CB2. Ann N Y Acad Sci 996:10–16. doi:10.1111/j.1749-6632.2003.tb03227.x

Klein TW, Cabral GA (2006) Cannabinoid-induced immune suppression and modulation of antigen-presenting cells. J NeuroImmune Pharmacol 1(1):50–64. doi:10.1007/s11481-005-9007-x

Klein TW, Newton C, Larsen K, Lu L, Perkins I, Nong L, Friedman H (2003) The cannabinoid system and immune modulation. J Leukoc Biol 74(4):486–496. doi:10.1189/jlb.0303101

Maccarrone M, Bab I, Biro T, Cabral GA, Dey SK, Di Marzo V, Konje JC, Kunos G, Mechoulam R, Pacher P, Sharkey KA, Zimmer A (2015) Endocannabinoid signaling at the periphery: 50 years after THC. Trends Pharmacol Sci 36(5):277–296. doi:10.1016/j.tips.2015.02.008

McKallip RJ, Lombard C, Martin BR, Nagarkatti M, Nagarkatti PS (2002) Delta(9)-tetrahydrocannabinol-induced apoptosis in the thymus and spleen as a mechanism of immunosuppression in vitro and in vivo. J Pharmacol Exp Ther 302(2):451–465. doi:10.1124/jpet.102.033506

Pacher P, Bátkai S, Kunos G (2006) The endocannabinoid system as an emerging target of pharmacotherapy. Pharmacol Rev 58(3):389–462. doi:10.1124/pr.58.3.2

Pérez-Gómez E, Andradas C, Blasco-Benito S, Caffarel MM, García-Taboada E, Villa-Morales M, Moreno E, Hamann S, Martín-Villar E, Flores JM, Wenners A, Alkatout I, Klapper W, Röcken C, Bronsert P, Stickeler E, Staebler A, Bauer M, Arnold N, Soriano J, Pérez-Martínez M, Megías D, Moreno-Bueno G, Ortega-Gutiérrez S, Artola M, Vázquez-Villa H, Quintanilla M, Fernández-Piqueras J, Canela EI, McCormick PJ, Guzmán M, Sánchez C (2015) Role of cannabinoid receptor CB2 in HER2 pro-oncogenic signaling in breast cancer. J Natl Cancer Inst 107(6):djv077. doi:10.1093/jnci/djv077

Rayman N, Lam KH, Laman JD, Simons PJ, Löwenberg B, Sonneveld P, Delwel R (2004) Distinct expression profiles of the peripheral cannabinoid receptor in lymphoid tissues depending on receptor activation status. J Immunol 172(4): 2111–2117. doi:10.4049/jimmunol.172.4.2111

Roth MD, Castaneda JT, Kiertscher SM (2015) Exposure to Δ9-Tetrahydrocanninol impairs the differentiation of human monocyte-derived dendritic cells and their capacity for T cell activation. J NeuroImmune Pharmacol 10:333–343. doi:10.1007/s11481-015-9587-z

Roth MD, Whittaker K, Salehi K, Tashkin DP, Baldwin GC (2004) Mechanisms for impaired effector function in alveolar macrophages from marijuana and cocaine smokers. J Neuroimmunol 147(1–2): 82–86. doi:10.1016/j.jneuroim.2003.10.017

Salazar M, Carracedo A, Salanueva IJ, Hernández-Tiedra S, Lorente M, Egia A, Vázquez P, Blázquez C, Torres S, García S, Nowak J, Fimia GM, Piacentini M, Cecconi F, Pandolfi PP, González-Feria L, Iovanna JL, Guzmán M, Boya P, Velasco G (2009) Cannabinoid action induces autophagy-mediated cell death through stimulation of ER stress in human glioma cells. J Clin Invest 119(5):1359–1372. doi:10.1172/JCI37948

Sarafian T, Kouyoumjian S, Khoshaghideh F, Tashkin DP, Roth MD (2003) Delta 9-tetrahydrocannabinol disrupts mitochondrial function and cell energetics. Am J Phys Lung Cell Mol Phys 284: L298–L306. doi:10.1152/ajplung.00157.2002

Sarafian T, Montes C, Harui A, Beedanagari SR, Kiertscher S, Stripecke R, Hossepian D, Kitchen C, Kern R, Belperio J, Roth MD (2008) Clarifying CB2 receptor-dependent and independent effects of THC on human lung epithelial cells. Toxicol Appl Pharmacol 231(3): 282–290. doi:10.1016/j.taap.2008.05.001

Schmöle AC, Lundt R, Gennequin B, Schrage H, Beins E, Krämer A, Zimmer T, Limmer A, Zimmer A, Otte DM (2015) Expression analysis of CB2-GFP BAC transgenic mice. PLoS One 10(9):e0138986. doi:10.1371/journal.pone.0138986

Yuan M, Kiertscher SM, Cheng Q, Zoumalan R, Tashkin DP, Roth MD (2002) Δ^9-Tetrahydrocannabinol regulates Th1/Th2 cytokine balance in activated human T-cells. J Neuroimmunol 133(1–2):124–131. doi:10.1016/S0165-5728(02)00370-3